

Effect of Impurity Puffing on Geodesic Acoustic Mode in OH and ECRH regimes on T-10

V.N. Zenin^{1, 2}, L.A. Klyuchnikov¹, A.V. Melnikov^{1, 3}, A.R. Nemets¹, M.R. Nurgaliev¹
and G.F. Subbotin^{1, 2}

¹ *NRC 'Kurchatov Institute', Moscow, Russia*

² *Moscow Institute of Physics and Technology, Dolgoprudny, Russia*

³ *National Research Nuclear University MEPhI, Moscow, Russia*

Physical mechanisms of the turbulent energy transport are actual topic in fusion research. Experiment shows that electrostatic potential plays an important role in plasma confinement and turbulent transport. Theory shows that zonal flows and its high-frequency counterpart the geodesic acoustic modes (GAMs), present the possible mechanism of the turbulence self-regulation [1]. GAMs primarily manifest themselves as oscillations of plasma electric potential and density. GAM frequency is proportional to the square root of temperature [2]. The main features of GAM in T-10 were described in [3]. The recent observations show that the edge plasma parameters play an important role in the GAM behavior [4].

T-10 is the circular tokamak ($R = 1.5$ m, $a = 0.3$ m, $B < 2.5$ T) with a rail carbon limiter. Plasma potential oscillations were studied with heavy ion beam probe (HIBP) [5, 6], a unique method of direct measurement of the electric potential in the hot plasma core. It has a high temporal (~ 1 ms) and spatial (~ 1 cm) resolution. Discharge scenario and the evolution of the main plasma parameters are presented in fig. 1. In regime with electron cyclotron heating (ECRH) after the short (~ 5 ms) He puffing the plasma periphery cools down, while the energy content and the line-averaged density shows some increase of about 10-15% and get the new steady state.

The fine details of the main plasma and GAM parameters are presented in fig. 2. Fourier spectrogram of potential oscillations, measured by HIBP is shown in fig. 2(a). GAM amplitude is shown in fig. 2(b). Just after the Helium pulse the GAM amplitude abruptly falls down during 2-5 ms. The GAM amplitude reaches minimum values and then evolves slowly to the new steady state with a characteristic time of about 70 ms, which is close to the density and temperature relaxation time. The evolution of GAM frequency is shown in fig. 2(c). It increases after the ECRH switch-on; then it decreases from ~ 17 kHz down to ~ 12 - 13 kHz

during ~ 25 ms after the He pulse, which is in a sharp contrast to the dynamics of the GAM amplitude.

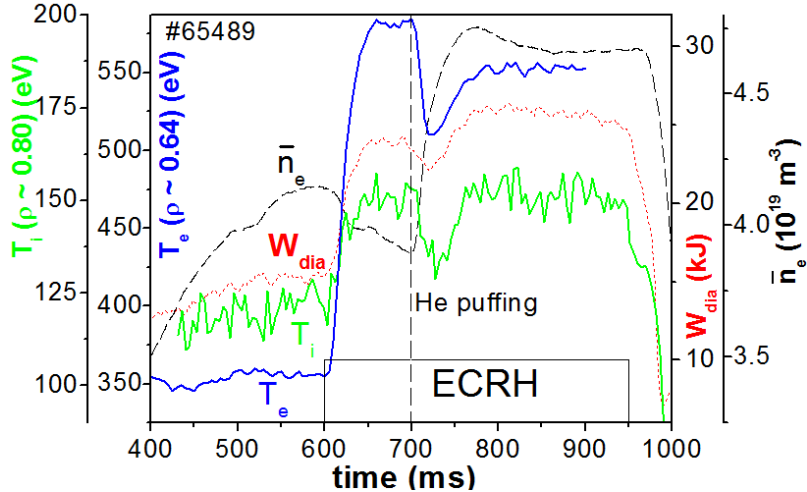


Figure 1. Scenario of the discharge with He puffing and the evolution of the main plasma parameters.

Here (n_e is the central chord line-averaged plasma density, T_e ($p=r/a = 0.64$) is the electron temperature, and T_i ($p= 0.80$) is the ion temperature, W_{dia} is the total stored energy.

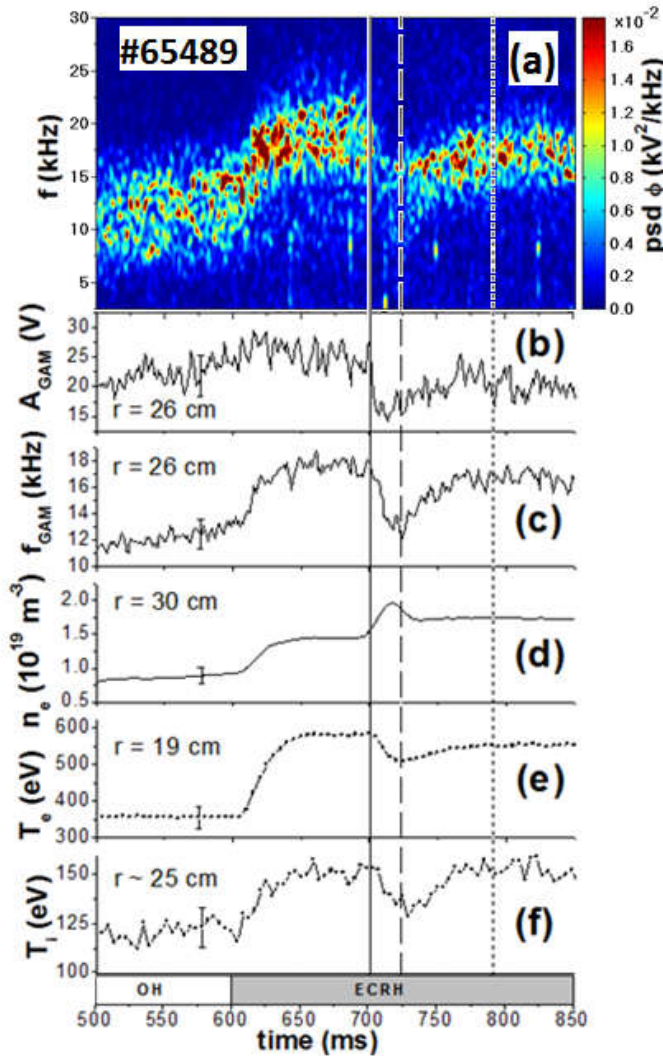


Figure 2. (a) — power spectrogram (power spectral density, psd) of potential oscillations, measured by HIBP at $r = 26$ cm, (b) — GAM amplitude, (c) — GAM frequency, (d) — electron density, measured by microwave interferometry at the edge chord, (e) — electron temperature, retrieved from the database of the electron cyclotron emission, (f) — ion temperature, measured by CXRS, (g) — density turbulence level, measured by correlation reflectometry. Both (f) and (g) were averaged over the series of identical shots (#65488 — 65492). Solid vertical line indicates He puffing, dash line — minimum of the GAM frequency, coinciding with a minimum of T_e , dot line — the steady state for GAM frequency

Besides, the mean potential is also affected by He pulse. The time traces of the plasma parameters are shown in figure 3. After ECRH switch-on the absolute value of plasma potential decreases in consistency with earlier observations [7]. Mean potential at the plasma periphery ($\rho > 0.8$) decreases right after the He pulse by 40-50 V during 30-35 ms. Then it recovers and reaches a new quasi steady-state level for $t=800$ -900 ms. This new level of absolute potential appears to be slightly higher than the initial stationary level before He puffing.

GAM dynamics has also been investigated for various impurity type like He, N, Ne. The main features of plasma potential and GAM evolution shows basically similar behaviour: sharp decrease of the GAM amplitude just after the impurity pulse. The similar decreasing of GAM amplitude also can be observed in OH regimes.

There is some MHD activity at 6-10 kHz, which is close to the GAM frequency range in the considered discharges. To select the GAM we have used the signal Z_d of HIBP that linked with poloidal magnetic field B , as shown in fig. 4.

In order to compare GAM frequency dependence with theoretical predictions [2] we estimated unavailable $T_e(\rho=0.8)$ at the plasma periphery as follows. To model $T_e(\rho=0.8)$ we use the time trace of $T_e(\rho=0.64)$, normalizes by ohmic value of $T_e(0.64)$. Here we assume the constancy of the T_e profiles on OH and ECRH phases of the discharge. Comparison between experimental data and theoretical estimates is shown in fig. 5 (GAM frequency is calculated over the region 10-25 kHz).

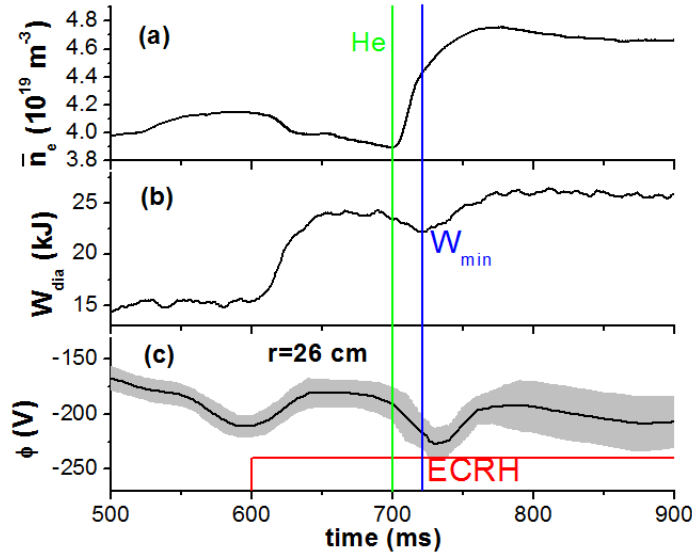


Figure 3. Evolution of electron density (a), stored energy (b) and plasma potential (c), grey shade represents experimental errors.

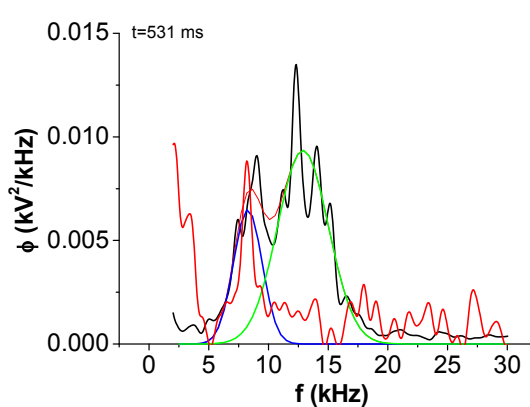


Figure 4. Comparison between spectra of $Zd \sim B$ and plasma potential

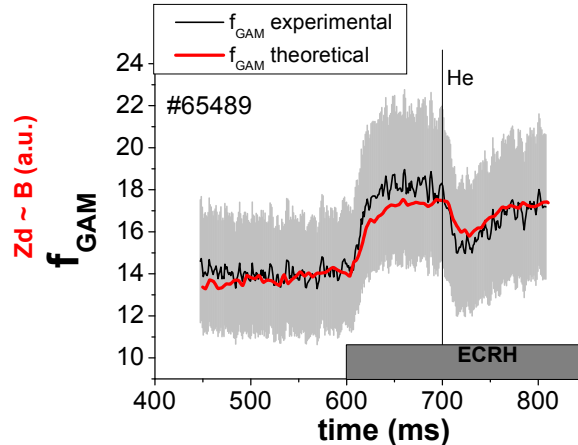


Figure 5. Comparison with theoretical predictions

Helium puffing dramatically changes the GAM behavior: GAM frequency decrease temporarily after the He pulse. GAM frequency evolution is consistent with the evolution of T_e and T_i at the plasma periphery. Unlike GAM frequency, the GAM amplitude reacts on He pulse abruptly (2-5 ms). Such sharp decrease can be probably linked with global character of GAM [6]. The further increase of GAM amplitude is consistent with collisional damping, caused by edge density evolution. GAM amplitude reduces sharply just after the impurity pulse.both in OH and ECRH regimes. Also this effect takes place after Ne and N₂ pulse. On top of that, the impurity pulse affects the mean plasma potential. Potential evolution mainly follows the density one and reveals its links with the energy content.

This work was funded by Russian Science Foundation, Project 14-22-00193.

References

- [1] Fujisawa A. *et al.* 2007 *Nucl. Fusion* **47**, S718–S726.
- [2] Winsor N., Johnson J. L., & Dawson J.M. 1968 *Phys. Fluids* **11**, 2448.
- [3] Melnikov A.V *et al.* 2006 *Plasma Phys. Control. Fusion* **48**, S87–S110.
- [4] Melnikov A.V. *et al.* 2015 *Nucl. Fusion* **55**, 063001.
- [5] Melnikov A.V. *et al.* 2013 *Nucl. Fusion* **53**, 093019.
- [6] Dnestrovskij, Yu.N. *et al.* 1994 *IEEE Trans. Plasma Sci.* **22**, 310–331.
- [7] Melnikov A.V. *et al.* 2011 *Nucl. Fusion* **51** 083043.